



Cranial Geometric Morphometric Analysis of the Genus *Tapirus* (Mammalia, Perissodactyla)

Larissa C. C. S. Dumbá¹ · Rodrigo Parisi Dutra^{1,2} · Mario A. Cozzuol³

Published online: 16 April 2018

© Springer Science+Business Media, LLC, part of Springer Nature 2018

Abstract

Tapirs are perissodactyl ungulates of the genus *Tapirus*. The family Tapiridae was more diverse in the past. Genus *Tapirus* include five living species: *T. indicus*, *T. pinchaque*, *T. bairdii*, *T. terrestris*, and *T. kabomani*. Despite all the information available about tapirs, evolutionary relationships among species within the genus are still uncertain. Recent works suggest that *T. terrestris* may be a species complex. A better understanding of the evolutionary history of this clade is essential to better support conservation strategies for the species of this genus, which are keys in the dynamics of tropical forests in Southeast Asia and Central and South America. Geometric morphometry has been proved to be a useful tool for the study of morphological evolution in mammals, but studies involving cranial geometric morphometry of tapiroids have never been done. We hereby propose landmarks for the study of tapir cranial shape through 2D geometric morphometric technique, including 20 in lateral cranial view ($n = 71$), 14 in dorsal cranial view ($n = 51$), and 21 in ventral cranial view ($n = 44$), followed by PCA multivariate statistical analysis that ordinated specimens from each of the three data groups along the major axis of shape variation. Lateral and dorsal view landmarks proved to be the most diagnostic for the species studied, providing interesting insights and trends on tapiroid cranial evolution. Ventrally, the species analyzed do not differentiate significantly. In this paper, we add new information to the current cranial morphometric database of tapirs, which can help elucidate questions about their evolutionary history.

Keywords *Tapirus* · Skull · Shape · Evolution · Geometric morphometry

Introduction

The genus *Tapirus* Brisson, 1762, includes five living species that occupy fragmented regions in South America, Central America, and Southeast Asia: in the first continent are

Electronic supplementary material The online version of this article (<https://doi.org/10.1007/s10914-018-9432-2>) contains supplementary material, which is available to authorized users.

✉ Larissa C. C. S. Dumbá
larissa.dumba@gmail.com

¹ PPG – Programa de Pós-Graduação em Zoologia/Departamento de Zoologia – Instituto de Ciências Biológicas, Universidade Federal de Minas Gerais, Avenida Antônio Carlos 6627, Belo Horizonte, Minas Gerais, Brazil

² Instituto de Engenharia e Tecnologia, Centro Universitário de Belo Horizonte, Avenida Professor Mário Werneck 1685, Belo Horizonte, Minas Gerais, Brazil

³ Departamento de Zoologia – Instituto de Ciências Biológicas, Universidade Federal de Minas Gerais, Avenida Antônio Carlos 6627, Belo Horizonte, Minas Gerais, Brazil

T. pinchaque (Roulin, 1829) of the Andes mountains, *T. terrestris* (Linnaeus, 1758) the lowland tapir, and *T. kabomani* Cozzuol et al., 2013, recently described for the the Amazon (Cozzuol et al., 2013, 2014), followed by *T. bairdii* (Gill, 1865) in Central and northern South America. *Tapirus indicus* Desmarest, 1819, inhabits fragmented regions in southeastern Asia. Several extinct species have been described for the genus (Hulbert 2010; Holanda and Ferrero 2012; Xue-Ping et al. 2015; Zlatozar 2017). The genus requires a comprehensive review of all species to clarify its content and definition. For now, we follow the definition of genus *Tapirus* as the clade including the most recent common ancestor of *Tapirus johnsoni* Schultz et al. 1975, which is considered the most primitive tapir species of the genus (Holanda and Ferrero 2012; Cozzuol et al. 2013, 2014). South American tapirs dispersed from North America during the Great American Biotic Interchange, which followed the formation of the Isthmus of Panama (Woodburne 2010; Cione et al. 2015; O’dea et al. 2016). Tapirs are browsing herbivores, feeding mainly on terrestrial and aquatic plants, leaves, and fruits. Being granivores and seed

dispersers, they play important roles in the dynamics of tropical forests (Olmos 1997). The tapir upper lip and flashy nose are long and prehensile, forming a proboscis (Padilla and Dowler 1994).

Cranial characters are highly diagnostic in mammals and skulls are the most common skeletal structures preserved in museum collections. Therefore, they are valuable tools for evolutionary studies; hence these were the structures chosen for this paper. The goal of this study is to better understand the cranial variation and its evolution among tapirs, including some relevant extinct species. Previous works demonstrated that skull shape varies considerably among living species of *Tapirus* (Holanda et al. 2011; Cozzuol et al. 2013, 2014). This paper aims to analyze skull shape variation between the five living tapir species and several extinct tapiroid species with geometric morphometry techniques, which have been widely used in the past few years for shape studies (Bookstein 1991; Marcus et al. 1996; MacLeod and Forey 2001; Zelditch et al. 2004). Although traditional morphometry describes the covariation pattern amongst all measurements and identifies regions with more or less covariation degree through the use of linear (distance) variables, it does not capture information regarding the shape of an organism as a whole as geometric morphometry does. Besides, geometric morphometry locates more clearly the regions of changes in shape and above all, it is able to construct and reconstruct these differences graphically (Morales 2003), and it has greater statistical robustness (Fornel and Cordeiro-Estrela 2012).

Geometric morphometry relies on shape acquisition and quantification through the establishment of homologous Cartesian coordinates called landmarks, rather than using linear variables (Monteiro and dos Reis 1999; Webster and Sheets 2001; Lawing and Polly 2010). Here, we choose 2D geometric morphometry as our technical approach to the study of cranial shape in tapirs. We apply those techniques to a tapiroid skull database in lateral, dorsal, and ventral views. In this analysis, we include all five living tapir species and several South and North American extinct species, besides two species representing two genera other than *Tapirus*: the tapiroid *Nexuotapirus marslandensis* Schoch and Prins in Schoch, 1984, and *Heptodon posticus* Cope, 1882, the phylogenetic position of which will be discussed below. These two genera were chosen inside Tapiroidea because they both have specimens suitable for morphometric analysis, attending to all the landmarks we hereby propose. Furthermore, as they are both tapiroids, a morphometric study of their skull shape may offer interesting insights on primitive and apomorphic characteristics retained by that group.

Concerning the genus *Nexuotapirus* Albright, 1984, it has an unclear phylogenetic position, as it exhibits numerous primitive and derived states of cranial characters. Some of the tapiroid plesiomorphic characters that the taxon carries are the extension of the lambdoidal crests posteriorly beyond the

occipital condyles, the confinement of the incisive foramina to the anteriormost part of the rostrum, and non-molariform upper premolars (Albright 1998). The derived cranial features that *Nexuotapirus* shares with tapirs are a deeply retracted nasal incision and shortened nasals and shortened frontals (Albright 1998). Regarding *Heptodon* Cope, 1882, it was included in a monophyletic Tapiroidea by Holbrook (1998) and as a derived tapiromorph species by Bai et al. (2014). As Holbrook's phylogenies were based on a larger number of tapiromorph groups and specimens, we hereby follow his attribution of *Heptodon* and the family Heptodontidae within the superfamily Tapiroidea as a basal tapiroid clade. Dasheveg and Hooker (1997) also placed *Heptodon* within the Tapiroidea.

About forty million years of evolution separates the basal tapiroid *Heptodon* from *Tapirus*, and the most notable cranial characteristics that distinguish them are modifications in the skull correlated with the development of a proboscis, such as the great enlargement of the nasal incision and a shortening of the nasals (Radinsky 1965). Less drastic cranial modifications that occurred between *Heptodon* and *Tapirus* involve dental evolution: premolars are not molarized in *Heptodon*, a primitive condition for tapiroids, as all extant and most extinct tapirs exhibit molarized premolars (except for PM1). By the end of the Oligocene (25 Ma), the evolutionary changes that resulted in the modern tapiroid skull were essentially completed, and since then there has been limited cranial evolution in the Tapiridae in general (Radinsky 1965).

Material and Methods

Samples Data for geometric morphometric analysis, including skull samples and pictures, were obtained from previous works (Radinsky 1965; Albright 1998; Ferrero and Noriega 2007; Hulbert et al. 2009; Hulbert 2010; Holanda et al. 2011) and specimens from several museum collections (a list of specimens analyzed in this paper follows in the Online Resource section 4 of this paper). Our data included three data groups, a lateral, a dorsal, and a ventral view group of skull pictures containing their own set of landmarks. Twenty lateral view landmarks (Fig. 1) were placed onto a total of 71 skull specimens of 11 tapiroid species: the extant *T. terrestris* (45 specimens), *T. indicus* (four specimens), *T. kabomani* (six specimens), *T. bairdii* (two specimens), and *T. pinchaque* (seven specimens), and the extinct *T. lundeliusi* Hulbert, 2010 (two specimens), *Heptodon posticus*, *Nexuotapirus marslandensis*, *T. johnsoni*, *T. mesopotamicus* Ferrero and Noriega, 2007, and *T. veroensis* Sellards, 1918 (all of them with one specimen each). Fourteen dorsal view landmarks (Fig. 2) were applied to a total of 51 tapiroid skull specimens distributed through ten species: the living species *T. terrestris* (28 specimens), *T.*

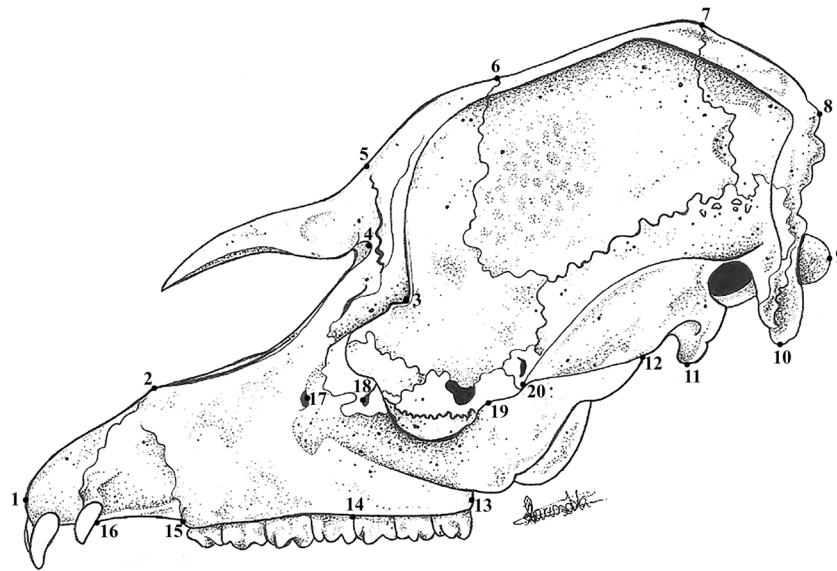


Fig. 1 Twenty cranial landmarks for the lateral view of the skull used in morphometric multivariate analysis: 1: Rostral tip of premaxilla; 2: Dorsal border of premaxilla-maxilla suture, lateral view; 3: Postorbital process of frontal; 4: Posterior margin of nasal opening; 5: Naso-frontal suture; 6: Fronto-parietal suture; 7: Parieto-occipital suture; 8: Posterior extremity of supraoccipital bone; 9: Posterior tip of occipital condyle; 10:

Tip of paroccipital process; 11: Posterior border of glenoid cavity; 12: Posterior end of jugal-squamosal suture; 13: Posterior end of dental series; 14: Premolar / molar limit; 15: Anterior border of P1 alveolus; 16: Posterior margin of canine alveolus; 17: Posterior end of infraorbital foramen; 18: Posterior process of lacrimal bone; 19: Postorbital process of the jugal; 20: Anterior end of jugal-squamosal suture

kabomani (six specimens), *T. pinchaque* (five specimens), *T. indicus* (four specimens), and *T. bairdii* (two specimens), and the extinct *T. lundeliusi* (two specimens), *T. veroensis*, *T. mesopotamicus*, *Nexutapirus marslandensis*, and *Heptodon posticus* (every one of these species with one specimen each). Lastly, 21 ventral view landmarks (Fig. 3) were studied in 44 specimens, including nine tapiroid species: *T. terrestris* (23 specimens), *T. kabomani* (five specimens), *T. pinchaque* (two specimens), *T. indicus* (two

specimens), *T. lundeliusi* (two specimens), *T. bairdii*, *T. veroensis*, *Nexutapirus marslandensis*, and *Heptodon posticus* (all species with one specimen analyzed).

Photographs taken for geometric morphometric analysis followed the same procedure of mounting, illumination, and image procurement (Webster and Sheets 2001; Zelditch et al. 2004) so that pictures resulted in appropriate material for the study of reliable landmark data. The camera used was a Fujifilm 12 MP with a focal distance of 5–90 mm, auto-

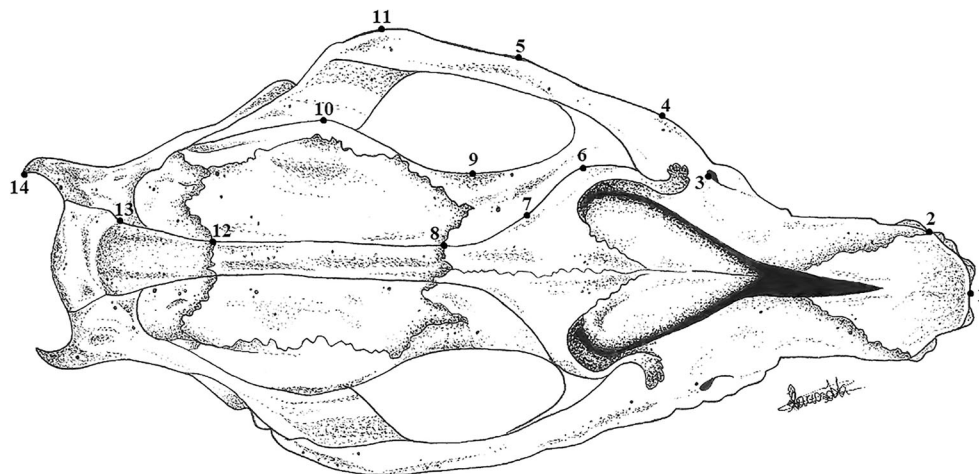


Fig. 2 Fourteen cranial landmarks for the dorsal view of the skull used in morphometric multivariate analysis: 1: Anteriormost rostral point of premaxilla; 2: Anterior border of canine alveolus; 3: Posterior border of infraorbital foramen; 4: Anterior end of jugal; 5: Lateral border of jugal at level of postorbital process of jugal; 6: Fronto-lateral border at level of naso-frontal suture; 7: Midpoint between landmarks 6 and 8 on

parasagittal ridge; 8: Fronto-parietal suture; 9: Maximum orbital constriction point in fronto-sphenoidal suture; 10: Lateralmost point of braincase at squamosal base; 11: External border of squamosal at level of anterior border of glenoid cavity; 12: Parieto-occipital suture; 13: Lambdoidal crest origin; 14: Posterior end of supraoccipital

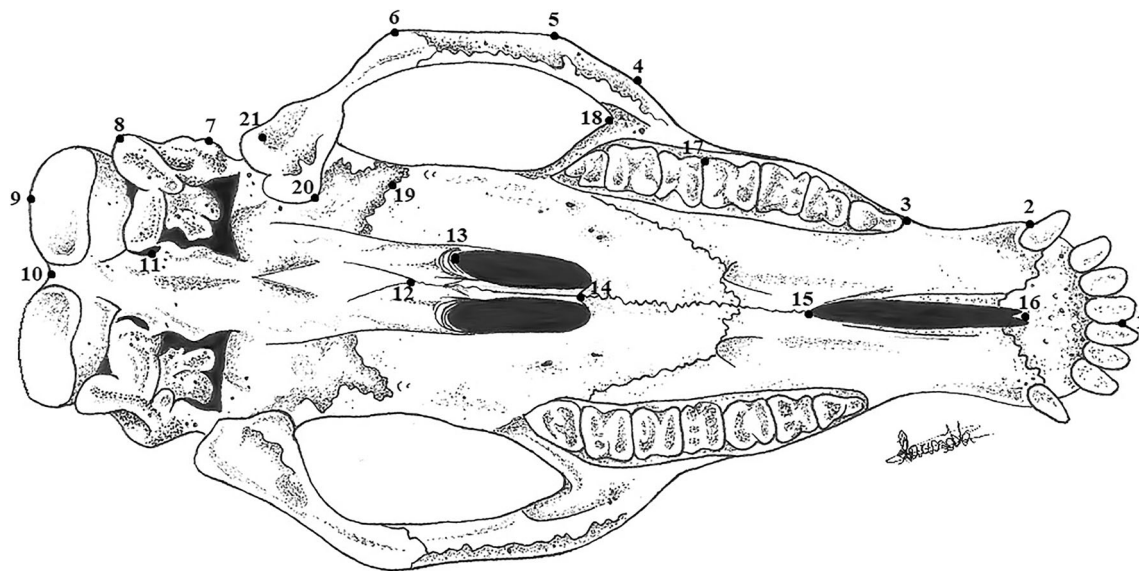


Fig. 3 Twenty one cranial landmarks for the ventral view of the skull used in morphometric multivariate analysis: 1: Anterior end of premaxilla; 2: Posterior border of canine alveolus; 3: Anterior border of P1 alveolus; 4: Anterior end of jugo-maxillary suture; 5: Lateral border of jugal at level of postorbital process of jugal; 6: Posteriormost point of jugal-squamosal suture; 7: Mastoid process; 8: Paraoccipital process; 9: Posteriormost point of occipital condyle; 10: Midpoint between

basioccipital condyles; 11: Hypoglossal foramen; 12: Presphenoid-basisphenoid suture; 13: Posterior border of choana; 14: Anterior border of choana at inter-palatine suture; 15: Posterior border of anterior palatine foramen; 16: Anterior border of anterior palatine foramen; 17: External border of the alveoli at premolar-molar border; 18: Posteriormost point of zygomatic process of maxilla; 19: Lateral extension of pterygoids; 20: Anterior border of glenoid cavity; 21: Postglenoid process

focus and lens opening of 3.1–5.6. The tooththrow was placed parallel to the base where the skull was positioned, so that all orientations of the photographs taken were the same for every specimen, reducing possibilities of intra- and interspecific skull shape variation due to poorly positioned specimens. The camera distance to every specimen was 1 m, so that parallax effect was avoided by not placing the skull too close to the camera (Mullin and Taylor 2002). Each specimen was positioned in the center of the picture, and a tripod was used to ensure camera stability during photography.

Geometric Morphometric Analysis Taxonomists use morphometry to quantitatively estimate differences in form between organisms, creating bases for comparisons and inferences of possible causes that led to those differences in shape (Monteiro and dos Reis 1999). To quantify and analyze those differences in geometric morphometry, landmarks are to be put onto the shape of interest. We selected points that satisfactorily covered and described skull shape. Landmarks are biologically homologous anatomical loci that are recognizable on all specimens in the study (Bookstein 1991). The points of reference acquired for this paper are located mostly in points of accepted homologies, such as those that are originated from unique shape patterns like tissue juxtaposition at bone sutures (Fornel and Cordeiro-Estrela 2012). Other landmarks described here represent points of considerable homology reliability, such as process ends, bone tips, and maximum curvature of structures (Fornel and Cordeiro-Estrela 2012).

Skull landmarks were acquired using the software TpsDig version 2.3, and were digitized in the same order for all specimens, as required by the program. As we were dealing with two dimensional (2D) geometric morphometric analyzes, this software created for each point of reference two coordinates in space ($x, y = 2D$). These 2D landmark coordinates were then exported to the software PAST version 2.14 (Hammer et al. 2001) and aligned using Generalized Procrustes Analysis (GPA, Rohlf and Slice 1990), a superimposition method that eliminates effects of scale, position, and orientation by centering configurations, leaving only shape as cause of variation inside the samples (Bookstein 1991).

Rescaling each configuration generates a common centroid size between all of them, meaning all differences in size and location were removed. GPA then generates a new matrix composed of new coordinates, called Procrustes, which are skull shape variables that can be statistically analyzed. The distance between two points in this multidimensional space represents how different these two shapes are: similar shapes are those that are close to each other and the most different ones are disposed far apart. Therefore, Procrustes distance is a way of measuring the differences between two or more shapes (Moraes 2003).

After superimposition, a multivariate Principal Components Analysis (PCA) associated with the disregard option, which doesn't force differences between groups, was performed with the software PAST version 2.14 (Hammer et al. 2001) to each one of the datasets, the first one including lateral cranial view landmarks (Fig. 1), the second consisting of cranial dorsal view

landmarks (Fig. 2), and the last one consisted of ventral view landmarks (Fig. 3). PCA is a statistical method that ordines specimens along the major axis of shape variation. The PC loadings obtained from PCA graphics are available in Online Resource section 5. As discussed in the “Results” section of this paper, ventral view landmarks were not diagnostic for the species analyzed, so we did not include them in the main text. The main PCA result generated from the analysis of ventral view landmarks is available in the Online Resource of this paper, section 3.

Concerning the lateral view landmarks acquired, photographs were taken from the left side of the skull as it is usually done for geometric morphometric studies, unless the left side was too damaged and missing reference points; in these cases photographs were taken of the right side of the skull. For dorsal view landmarks, only the left side of the skull was represented in order to reduce data redundancy, as tapirs are bilaterally symmetrical organisms (Webster and Sheets 2001). As acquired by geometric morphometric analysis, only skulls complete enough to take all landmarks were used. Only adults, tapirs in which at least M2 was fully erupted (Cozzuol et al. 2013, 2014), were photographed, meaning only interspecific differences are responsible for different skull shapes in the results, not growth. An exception, a *T. bairdii* with just the M1 erupted, a subadult and therefore sexually mature (Gibson 2011; Cozzuol et al. 2013, 2014), was included in the analysis because of the lack of skull samples of this species that are complete enough to

attend all landmarks acquired. The lack of samples of *T. indicus*, *T. bairdii*, and most of the extinct species available in museum collections interferes directly in our sample size of its species and consequently on our results. More data of these tapirs need to be collected so we can better understand how skull shape evolved inside *Tapirus*. The datasets generated and/or analyzed during the current study available from the corresponding author on reasonable request.

Results

PCA ordines specimens along the major axis of shape variation (Lawing and Polly 2010). From the PCA matrix produced by the analysis of the 20 lateral view landmark dataset ($n = 71$), PCs 1 to 5 explain 71% of total variance, and therefore they are the most representative of the variation between species analyzed. PC5 was excluded from the PCA analysis we generated because it explains alone very little of the total variation between groups, and it is near to noise effects. Because of that, the combinations between the first four PCs that better separated the species were the ones chosen and are shown in this paper (PC1 versus PC2 – Fig. 4; PC2 versus PC3 – Fig. 5; and PC2 versus PC4 – Fig. 6). Lastly, we generated a lateral landmark PCA matrix without *Heptodon posticus* to assess the effect of its exclusion, combining the

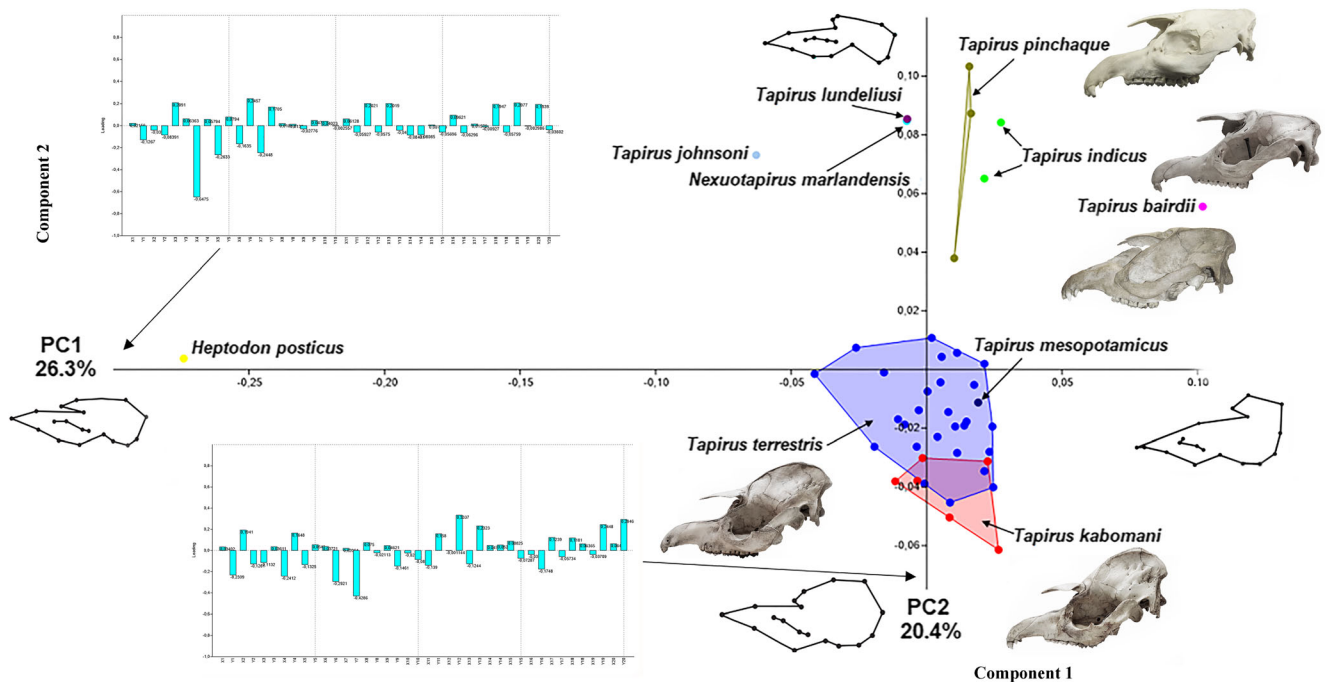


Fig. 4 Results of PCA diagram for 20 lateral view landmarks ($n = 71$) superimposed using GPA, PC1 versus PC2, for extant and extinct species of tapiroid species, mostly *Tapirus* species. PCA matrix includes the following extinct species: the tapiroid *Heptodon posticus* (yellow dot), the tapiroid *Nexuotapirus marlandensis* (flashy blue dot), *T. johnsoni*

(light-blue dot), *T. mesopotamicus* (dark blue dot), and *T. lundeliusi* (purple dot); and all extant species: *T. terrestris* (blue dots), *T. kabomani* (red dots), *T. bairdii* (light purple dot), *T. indicus* (green dots), and *T. pinchaque* (beige dots)

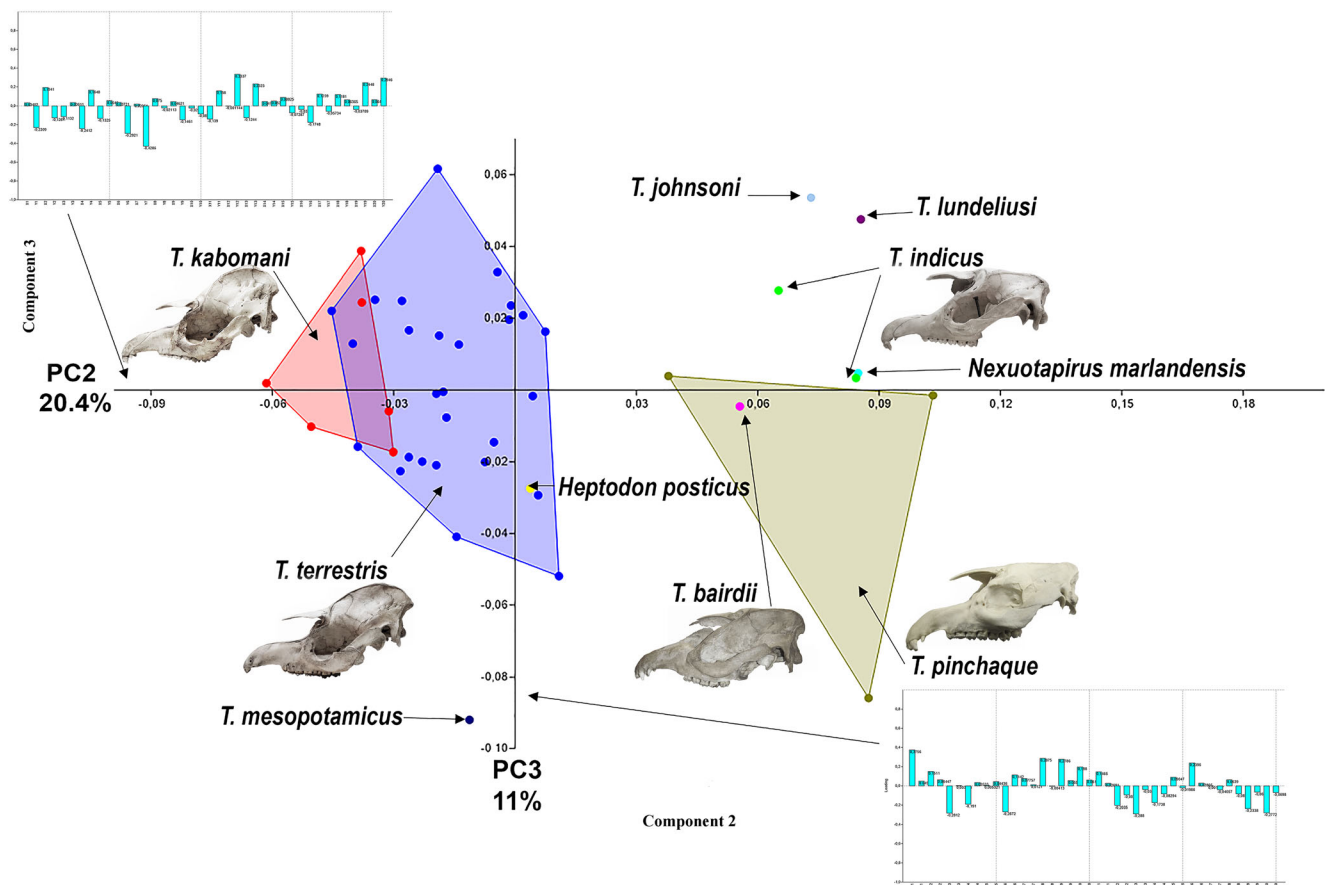


Fig. 5 Results of PCA diagram for 20 lateral view landmarks ($n=71$) superimposed using GPA, PC2 versus PC3, for extant and extinct species of tapiroid species, mostly *Tapirus* species. PCA matrix includes the following extinct species: the tapiroid *Heptodon posticus* (yellow dot), the tapiroid *Nexuotapirus marlandensis* (flashy blue dot), *T. johnsoni*

(light-blue dot), *T. mesopotamicus* (dark blue dot) and *T. lundeliusi* (purple dot); and all extant species: *T. terrestris* (blue dots), *T. kabomani* (red dots), *T. bairdii* (light purple dot), *T. indicus* (green dots), and *T. pinchaque* (beige dots)

first and second PCs (which explain 25% and 15% of the total variation, respectively) that formed the most diagnostic graphic (Online Resource 1). The removal of *Heptodon posticus* from the dorsal and ventral landmark analysis did not show a significant difference from those analysis in which this species was included.

For the analysis of the 14 dorsal view landmark PCA matrix ($n=51$), PCs 1 to 3 explain 74% of the total variance between species and therefore the combination between these PCs that better separated the species was chosen (PC1 versus PC3). As none of the PCs combinations including PC2 produced a diagnostic graphic for the data analyzed, but it is a significant PC in the final percentage of variation amongst species, the most diagnostic graphic containing PC2 can be seen in Online Resource section 2. None of the combinations between the first five PCs (which explain together 70% of the variation between species) generated by the analysis of the 21 ventral view landmarks ($n=44$) produced a diagnostic graphic. Therefore, we included only the most diagnostic graphic produced by the combination of the first two PCs, which

explain 21% and 18% of the total variation, respectively, inside Online Resource section 3.

Discussion

Lateral view landmarks proved to be the most diagnostic ones for the data analyzed, followed by dorsal view landmarks. Concerning lateral view landmarks, the first graphic (PC1 versus PC2, Fig. 4), PC1 loadings show that this PC is highly influenced by landmark 4, located in the posterior margin of the nasal opening (see Fig. 1). Therefore, all combinations of graphics including PC1 show species that are separated mainly because of landmark 4 position in their skull. As previously mentioned, nasal bone retraction is an osteological indicator of the presence of a proboscis in tapiirs, absent in *Heptodon*. This profile is understandable as *H. posticus* is a tapiroid, not a Tapiridae, and both *Tapirus* and *Nexuotapirus* belong to the latter taxon. The presence of an extensive nasal retraction, a reduction of the nasal cavity bone wall (Witmer et al. 1999), and an increased nasal notch (Wall 1980; Holbrook 1998) are

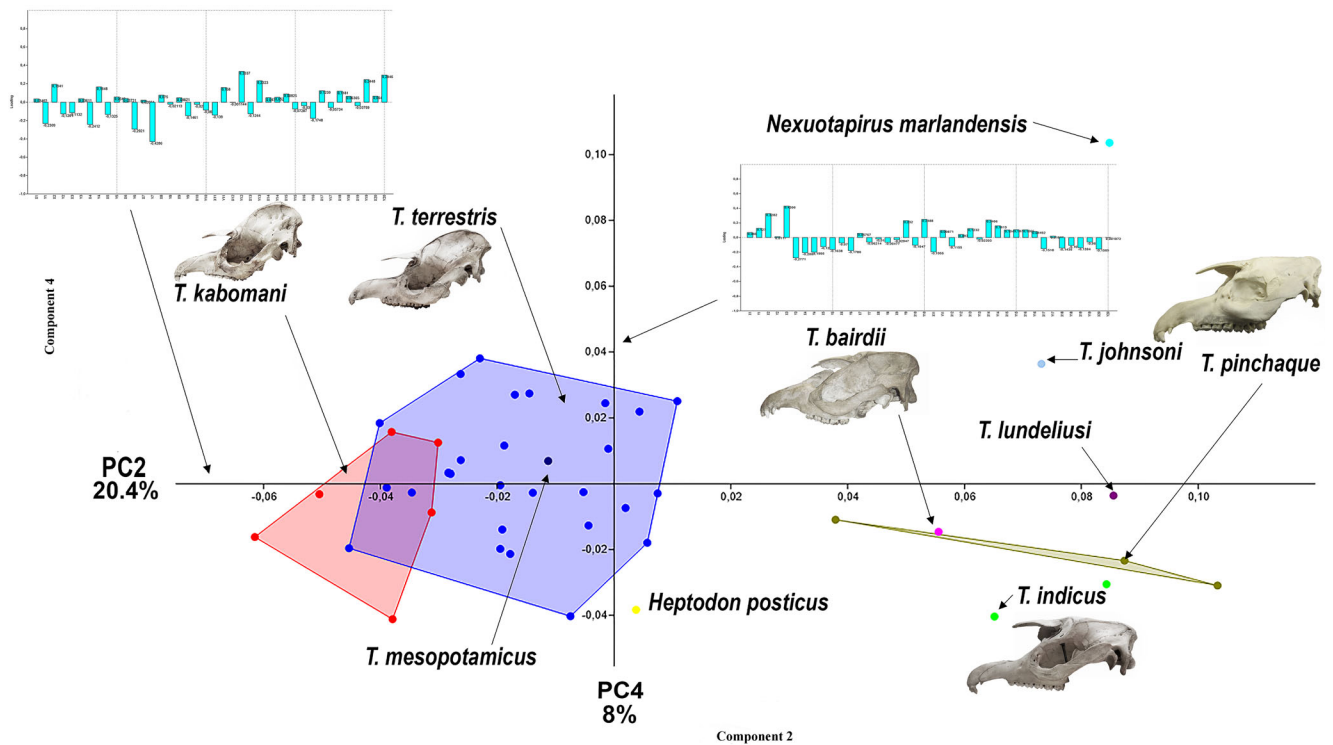


Fig. 6 Results of PCA diagram for 20 lateral view landmarks (n=71) superimposed using GPA, PC2 versus PC4, for extant and extinct species of tapiroid species, mostly *Tapirus* species. PCA matrix includes the following extinct species: the tapiroid *Heptodon posticus* (yellow dot), the tapiroid *Nexuotapirus marlandensis* (flashy blue dot), *T. johnsoni*

(light-blue dot), *T. mesopotamicus* (dark blue dot), and *T. lundeliusi* (purple dot); and all extant species: *T. terrestris* (blue dots), *T. kabomani* (red dots), *T. bairdii* (light purple dot), *T. indicus* (green dots), and *T. pinchaque* (beige dots)

osteological indicators of the development of a short and flexible proboscis, one of the most characteristic skull characters of tapirs and most tapiroids (Rustioni and Mazza 2001). As described by Radinsky (1965), the biggest differences between the skulls of *Heptodon* and tapirs are those associated with proboscis development. The absence of this organ is a primitive condition for Tapiroidea, as almost all tapiroids and all *Tapirus* possess a proboscis. Thus, it is expected that the position of landmark 4 (located at the posterior margin of the nasal opening) in tapirs is far more posterior to that of *Heptodon*, separating these two genera. This is confirmed by the analysis of our morphometric data, as it can be seen clearly when PC1 is included in the analysis (Fig. 4).

Besides the absence of osteological indicators of a proboscis, less drastic cranial modifications that separate tapirs from *Heptodon* are the ones that resulted from brain evolution. The braincase of *Heptodon* is relatively shorter than that of tapirs, probably as a result of cerebral expansion, and sagittal and lambdoidal crests are relatively lower and do not project back as far in tapirs as in *Heptodon*, a characteristic that is probably primitive inside the genus *Tapirus* (Radinsky 1965). *Heptodon posticus* exhibit some other characteristics that are trusted to be primitive for tapiroids, such as the presence of a narial incision that is unretracted, absence of a nasolacrimal

contact, and a postglenoid process obliquely oriented (Holbrook 1998). In Online Resource 1, the graphic with *Heptodon posticus* removed increases the distances between the remaining species, with both PC1 and PC2 being useful axes to discriminate most of them, which implies that tapiroids skull are still morphometrically different. *Nexuotapirus marlandensis* is a tapiroid that probably had a proboscis, as its skull exhibits nasal retraction, a factor that appears to separate the most the species in this graphic as mentioned in the last paragraph. As this species falls next to the tapir species in this analysis, and far apart from *Heptodon posticus*, it is an indicator that *Nexuotapirus marlandensis* likely did possess a mobile proboscis.

Although the presence or absence of a proboscis may be the most influential factor for diagnosis in Fig. 4, some other observations can be made about the general aspect of this result. Still inside the PCA of PC1 and 2, there is a clear discrimination between almost all species, with a considerable overlap between *Nexuotapirus marlandensis* and *T. lundeliusi*, and disposed close to them in the matrix are *T. johnsoni* and *T. pinchaque*. These four species exhibit similar cranial shape, including a dorso-ventrally flattened skull, elongated rostrum, and sagittal crest extending straight to the nasals. Furthermore, *T. johnsoni*, *T. lundeliusi*, and

T. pinchaque exhibit elongated nasals, a condition referred as primitive inside *Tapirus* (Hulbert 2010). The cranial similarities shared by those three tapir species are probably homoplasies, as none of them are closely related inside recent phylogenetic hypothesis (Holanda and Ferrero 2012; Cozzuol et al. 2013, 2014). Besides relatively elongated nasals, the other primitive skull features of *T. lundeliusi* are the presence of a reduced maxillary edge and a narrow lacrimal bone (Hulbert 2010). Still inside this group, the late Miocene species *T. johnsoni*, which was referred as probably being the most basal tapir (Holanda and Ferrero 2012; Cozzuol et al. 2013, 2014), has a more anteriorly located mental foramen as another primitive cranial characteristic for the genus *Tapirus*.

Tapirus indicus and *T. bairdii* are close to each other in the lateral view landmark PCA matrix, varying the most along the PC2 axis. Both possess a dorso-ventrally extended skull, both of them have a deep and extensive fossa on the dorsal surface of the nasal, and the frontal houses the meatal diverticulum (Hulbert 2005). These two species also have broad frontals, and this characteristic seems to be primitive inside the genus *Tapirus* (Holanda et al. 2011). The presence of broad nasals in both *T. indicus*, *T. bairdii*, and *T. terrestris* is probably a convergence as they do not share close relations (Holanda and Ferrero 2012; Cozzuol et al. 2013, 2014). *Tapirus terrestris* and *T. kabomani* exhibit some degree of overlap, although *T. kabomani* seems to vary the most along PC2 axis. Although *T. kabomani* and *T. terrestris* share some cranial similarities, they have notable differences, as noted in the inflated frontal bones that form a large triangular convex exposure in *T. kabomani*, ending posteriorly at the frontal–parietal suture, where the sagittal crest begins; in *T. terrestris* the sagittal crest extends more anteriorly than in *T. kabomani*, in the frontals (Cozzuol et al. 2013, 2014). Also in Fig. 4, *T. mesopotamicus* falls into *T. terrestris* variation. Characteristics that are present in both *T. mesopotamicus* and *T. terrestris* skulls in lateral view are a knobby posterior lacrimal process, a ventro-lateral edge of the maxilla that ends abruptly at the medial side of P1, a lateral or supraorbital groove for the nasal diverticulum leading up to the spiral grooves, which are deep and narrow, and lambdoidal crests that are strong, well separated, and projected posterior to the occipital condyles (Ferrero and Noriega 2007). However, a definite character that differentiates *T. mesopotamicus* from *T. terrestris* is the shape of the sagittal crest, with the latter showing a striking sagittal crest, a condition shown to be derived in tapirs (Ferrero and Noriega 2007).

As PC1 is profoundly influenced by landmark 4 and there are other significant PCs also explaining a considerable portion of the total variation between species for lateral view landmarks, as mentioned before, we generated two other graphics: one containing PC2 versus PC3 (Fig. 5) and the other one combining PC2 and PC4 (Fig. 6). They are not highly influenced by one specific landmark as PC1 is, so the combinations between PC2, 3, and 4 allow the observation of

skull shape differences between these species in a more consistently and less tendentious way. In Fig. 5, a PCA matrix scatterplot of PC2 and PC3, without considering the high influence caused by the position of landmark 4 in PC1 for the cranial shape between the species analyzed, *Heptodon* is not distant from tapirs: it actually falls inside *T. terrestris* skull shape variation. Results in Fig. 6 (a graphic combination of PC2 and 4) show a similar condition, with *H. posticus* falling next to the *T. terrestris* group. Therefore, our analysis indicates that with the exception of the nasal bone retraction, the skull of *H. posticus* is essentially like other tapirs.

As both of the graphics of Figs. 5 and 6 have a more homogeneous loadings distributions through their PCs than that of Fig. 4, no bone structure on the skull appears to have a distinct influence on the PCA matrix as it did on Fig. 4, showing that there is less disparity between the influences of all landmarks in shape variation. All cranial structures related to the landmarks acquired seem to contribute more equally to the diagnosis of the species in Figs. 5 and 6. The same general tendencies and observations discussed for grouping species next to each other in Fig. 4 can be observed in Figs. 5 and 6, with little differences observed. For example, as in Fig. 4, a dorso-ventrally flattened skull shared by *Nexuotapirus marlandensis*, *T. lundeliusi*, *T. johnsoni*, and *T. pinchaque* bring these taxa next to each other in Figs. 5 and 6 too, apparently because PC2 loadings are considerably influenced by landmark 7 (parietal-occipital suture), related to sagittal crest height and consequently to dorso-ventrally flattened or elongated skulls. This tendency can also be seen on the other side of the graphic, where animals with higher sagittal crests are displayed closer inside the matrix (*T. kabomani*, *T. terrestris*, and *Heptodon posticus*).

Concerning the dorsal landmark data, the most significant graphic produced by the analysis of the data was the one exhibiting the combination of PC1 and 3 (Fig. 7). PC2's loadings showed that this PC is mostly influenced by landmark 5 (external border of the jugal at the level of the postorbital process), and although it is a significant PC for explaining total variation among the species, it was not a diagnostic bone character for the species studied in this paper. For this reason, as mentioned before the graphic containing the best combination for a PC2 analysis (PC1 versus PC2) is included only in Online Resource section 2, but it will not be discussed here. In Fig. 7, PC1's loadings are highly influenced by landmarks 6 and 7 (frontal lateral border at the level of the nasal-frontal suture and midpoint between landmarks 6 and 8 on the parasagittal ridge, respectively), and PC3 is mostly influenced by landmarks 6 and 8 (landmark 8 stands in the frontal-parietal suture). It means that for our data, when analyzing the combination of the most significant PCs, the landmarks that contribute the most to better diagnose the group of species being studied are the ones that form tapiroids forehead. Thus, species that have similarly shaped foreheads are expected to fall next to

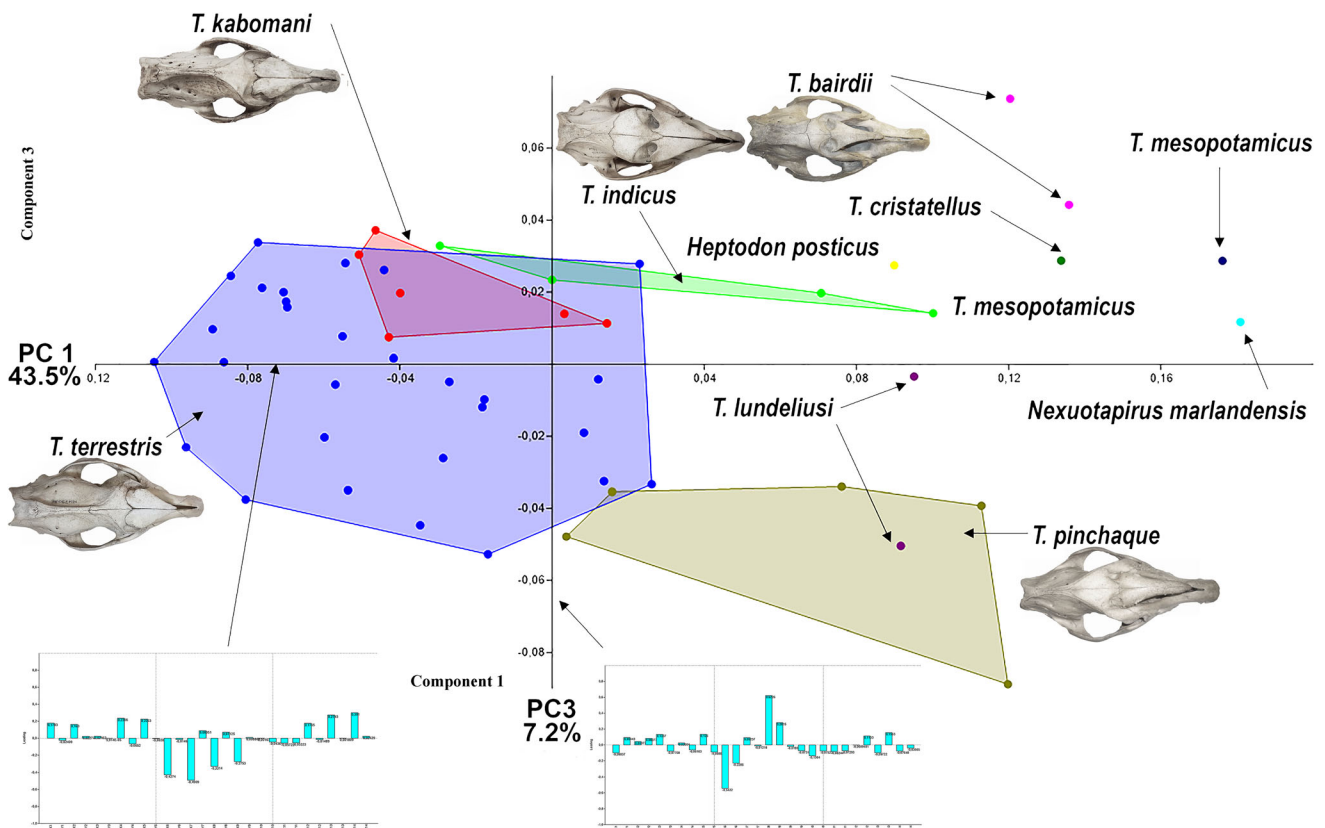


Fig. 7 Results of PCA matrix for 14 dorsal view landmarks ($n = 51$) superimposed using GPA, PC1 versus PC3, for extant and extinct species of Tapiridae species, mainly *Tapirus*. PCA matrix includes the extinct species *Heptodon posticus* (yellow dot), *Nexuotapirus marlandensis* (flashy blue dot), *T. mesopotamicus* (dark blue dot),

T. lundeliusi (purple dots), and *T. veroensis* (dark green dot); and all extant species: *T. terrestris* (blue dots), *T. kabomani* (red dots), *T. bairdii* (light purple dot), *T. indicus* (green dots), and *T. pinchaque* (beige dots)

each other in the PCA matrix. That is precisely what happened for a group formed in the right side of the graphic, composed of *Heptodon posticus*, *T. cristatellus*, *T. indicus*, and *T. bairdii*, all including species that have a broad forehead. In the extreme right of the PCA matrix are *T. mesopotamicus* and *Nexuotapirus marlandensis*, both possessing the broadest forehead state of all tapiroids studied in this paper, and a retraction of the sagittal crest, directly related to the position of the frontal-parietal suture (landmark 8), which was highly diagnostic for PC3 as mentioned before. A broad forehead is a primitive character for tapiroids, retained by those last mentioned species. Both *T. mesopotamicus* and *Nexuotapirus marlandensis* appear to have laterally compressed skulls, which seem to contribute to placing them next to each other as well. Although *T. pinchaque* and *T. lundeliusi* are close to each other, variation through *T. pinchaque* specimens is mostly horizontal in the graphic (through PC1), and the variation of *T. lundeliusi* goes especially through PC3, vertically. In the left side of the same matrix of Fig. 7, *T. kabomani* falls considerably superimposed to *T. terrestris*. These are the two species with the longest sagittal crests (directly influenced by landmark 8). *Tapirus kabomani* exhibits the broadest forehead of these two species, and apparently because of that it falls slightly

more to the right of the graphic. *Tapirus terrestris* possesses a sagittal crest that extends onto the frontals, a characteristic that is believed to be derived for *Tapirus*, and could have contributed to its distribution along PC3 axis.

Conclusions

The results support our hypothesis of interspecific variation in cranial shape between the tapir, tapirid, and tapiroid species analyzed. PCA analysis of a tapir cranial geometric morphometric dataset not only demonstrated how different living and extinct tapiroid skull species are, but also allowed identification and discrimination of distinct morphological groups, based on skull similarities that they share. Analysis of our data also permits the formulation of interesting evolutionary trends for tapiroids. Our study corroborates previous analyses of cranial shape diversity among tapirs, allocating species that have been described previously as having similar cranial shape next to each other on the PCA matrix, demonstrating that geometric morphometric techniques may be helpful for better understanding how the tapir skull evolved. Our results show that lateral view skull shape is the one that varies the most amongst

extant and extinct tapir species, with at least three combinations of the most significant PCs exhibiting a great degree of interspecific variation. When eliminating the high influence of the retraction of the nasal bone present in PC1, *Heptodon posticus* appears to have a similar skull shape to that of other tapirs, confirming previous works (Radinsky 1965) that stated that aside from the osteological differences associated with the development of a proboscis, the tapir skull has changed little since early tapiroids. This morphometric information may help enforcing the position of *Heptodon* as a tapiroid and not as a basal tapiromorph. Dorsally, skull shape appears to be diagnostic for PC1 and 3, and they are highly influenced by landmarks that are part of the forehead and the sagittal crest, indicating that those cranial structures were the most diagnostic for the species analyzed. Ventral skull shape analysis shows the highest overlap rate between species, indicating that the species studied have no significant ventral skull shape differences.

Acknowledgements This work received grants from FAPEMIG and CAPES from Brazil. We thank C. Cartelle (Museu de Ciências Naturais PUC Minas, Belo Horizonte, Brazil), L. F. B. Flamarion (Coleção de Mastozoologia do Museu Nacional do Rio de Janeiro, Brazil), and F. A. Perini (Coleção de Mastozoologia da Universidade Federal de Minas Gerais, Belo Horizonte, Brazil) for the access to tapir collections.

References

- Albright LB (1998) New genus of tapir (Mammalia: Tapiridae) from the Arikareean (earliest Miocene) of the Texas Coastal Plain. *J Vertebr Paleontol* 18:200–217
- Bai B, Wang Y, Meng J, Li Q, Jin X (2014) New early Eocene basal tapiromorph from southern China and its phylogenetic implications. *PLoS One* 9(10):e110806
- Bookstein FL (1991) *Morphometric Tools for Landmark Data: Geometry and Biology*. Cambridge University Press, Cambridge
- Cione AL, Gasparini GM, Soibelzon E, Soibelzon LH, Tonni EP (2015) The Great American Biotic Interchange. A South American Perspective. SpringerBriefs in Earth System Sciences. Springer, Dordrecht
- Cozzuol MA, Clozato CL, Holanda EC, Rodrigues FHG, Nienow S, de Thoisy B, Redondo RAF, Santos FR (2013) A new species of tapir from the Amazon. *J Mammal* 94:1331–1345
- Cozzuol MA, de Thoisy B, Fernandes-Ferreira H, Rodrigues FHG, Santos FR (2014) How much evidence is enough evidence for a new species? *J Mammal* 95:899–905
- Dashevsk D, Hooker JJ (1997) New ceratomorph perissodactyls (Mammalia) from the middle and late Eocene of Mongolia: their implications for phylogeny and dating. *Zool J Linn Soc* 120:105–138
- Ferrero B, Noriega JI (2007) A new upper Pleistocene tapir from Argentina: remarks on the phylogenetics and diversification of Neotropical Tapiridae. *J Vertebr Paleontol* 27:504–511
- Fornel R, Cordeiro-Estrela P (2012) Morfometria Geométrica e a quantificação da forma nos organismos - Temas em Biologia: Edição Comemorativa aos 20 anos do Curso de Ciências biológicas e aos 5 anos do PPG-Ecologia da URI Campus Erechim. PPG-Ecologia, Erechim
- Gibson ML (2011) Population structure based on age-class distribution of *Tapirus polkensis* from the Gray Fossil Site Tennessee. M.S. Thesis, East Tennessee State University, Johnson City
- Hammer Ø, Harper DAT, Ryan PD (2001) PAST: paleontological statistics software package for education and data analysis. *Palaeontol Electronica* 4:1–9
- Holanda EC, Ferigolo J, Ribeiro AM (2011) New *Tapirus* species (Mammalia: Perissodactyla: Tapiridae) from the upper Pleistocene of Amazonia, Brazil. *J Mammal* 92:111–120
- Holanda EC, Ferrero B (2012) Reappraisal of the genus *Tapirus* (Perissodactyla, Tapiridae): systematics and phylogenetic affinities of the South American tapirs. *J Mammal Evol* 20:33–44
- Holbrook LT (1998) The phylogeny and classification of tapiromorph perissodactyls (Mammalia). *Cladistics* 15:331–350
- Hulbert RC Jr (2005) Late Miocene *Tapirus* (Mammalia, Perissodactyla) from Florida, with description of a new species, *Tapirus webbi*. *Bull Florida Mus Nat Hist* 45:465–494
- Hulbert RC Jr (2010) A new early Pleistocene tapir (Mammalia: Perissodactyla) from Florida, with a review of Blancan tapirs from the state. *Bull Florida Mus Nat Hist* 49(3):67–126
- Hulbert RC Jr, Wallace SC, Klippel WE, Parmalee PW (2009) Cranial morphology and systematics of an extraordinary sample of the late Neogene dwarf tapir, *Tapirus polkensis* (Olsen). *J Paleontol* 8:238–262
- Lawing AM, Polly PD (2010) Geometric morphometrics: recent applications to the study of evolution and development. *J Zool* 280:1–7
- Marcus LF, Corti M, Loy A, Naylor GJP, Slice DE (1996) *Advances in Morphometrics*. Plenum, New York
- MacLeod N, Forey PL (2001) *Morphology, Shape, and Phylogeny*. Taylor and Francis, London
- Monteiro L, dos Reis SF (1999) *Princípios de morfometria geométrica*. Holos Editora, Ribeirão Preto
- Moraes DA (2003) A morfometria geométrica e a “revolução na morfometria”: localizando e visualizando mudanças nas formas dos organismos. *Bioletim*, São Paulo
- Mullin SK, Taylor PJ (2002) The effects of parallax on geometric morphometric data. *Computers in Biology and Medicine* 32:455–464
- O’Dea A, Lessios HA, Coates AG, Eytan RI, Restrepo-Moreno SA, Cione AL, Stallard RF, Collins LS, de Queiroz A, Farris DW, Norris RD, Stallard RF, Woodburne MO, Aguilera O, Aubry MP, Berggren WA, Budd AF, Cozzuol MA, Coppard SE, Duque-Caro H, Finnegan S, Gasparini GM, Grossman EL, Johnson KG, Keigwin LD, Knowlton N, Leigh EG, Leonard-Pingel JS, Marko PB, Pyenson ND, Rachello-Dolmen PG, Soibelzon E, Soibelzon L, Todd JA, Vermeij GJ, Jackson JB (2016) Formation of the Isthmus of Panama. *Sci Adv* 2:e1600883
- Olmos F (1997) Tapirs as seed dispersers and predators. In: Brooks DM, Bodmer RE, Matola S (eds) *Tapirs—Status Survey and Conservation Action Plan*. IUCN Publications Services Unit, Cambridge, pp 3–9
- Padilla M, Dowler RC (1994) *Tapirus terrestris*. *Mammal Species* 481:1–8
- Radinsky LB (1965) Evolution of the tapiroid skeleton from *Heptodon* to *Tapirus*. *Bull Mus Comp Zool* 134:69–106
- Rohlf FJ, Slice D (1990) Extensions of the Procrustes method for the optimal superimposition of landmarks. *Syst Zool* 39(1):40–59
- Rustioni M, Mazza P (2001) Taphonomic analysis of *Tapirus arvenensis* remains from the lower Valdarano (Tuscany, central Italy). *Geobios* 34(4):469–474

- Wall WP (1980) Cranial evidence for a proboscis in *Cadurcodon* and a review of snout structure in the family Aymnodontidae (Perissodactyla, Rhinocerotidae). *J Paleontol* 54(5):968–977
- Webster M, Sheets HD (2001) A practical introduction to landmark-based geometric morphometrics. In: Alroy J, Hunt G (eds) *Quantitative Methods in Paleobiology*. *Palaeontol Soc Pap* 16:163–188
- Witmer LM, Sampson SD, Solounias N (1999) The proboscis of tapirs (Mammalia: Perissodactyla): a case study in novel narial anatomy. *J Zool* 249(3):249–267
- Woodburne MO (2010) The Great American Biotic Interchange: dispersals, tectonics, climate, sea level and holding pens. *J Mammal Evol* 17:245–264
- Xue-Ping JI, Jablonski NG, Hao-Wen T, Su DF, Ebbestad JOR, Cheng-Wu L, Teng-Song Y (2015) *Tapirus yunnanensis* from Shuitangba, a terminal Miocene hominoid site in Zhaotong, Yunnan Province of China. *Vertebr Palasiatica* 53:177–192
- Zlatozar B (2017) Fossil record of tapirs (*Tapirus* Brünnich, 1772) (Tapiridae Gray, 1821 - Peryssodactyla Owen, 1848) in Bulgaria. *ZooNotes* 108:1–3
- Zelditch ML, Swiderski DL, Sheets HD, Fink WL (2004) *Geometric Morphometrics for Biologists: A Primer*. Elsevier, Amsterdam